

## Supplementary Information for Mapping the magnetization fine structure of a lattice of Bloch-type skyrmions in an FeGe thin film

András Kovács,<sup>1, a)</sup> Jan Caron,<sup>1</sup> Andrey Savchenko,<sup>2</sup> Nikolai S. Kiselev,<sup>3, b)</sup>  
Kiyohi Shibata,<sup>4</sup> Zi-An Li,<sup>5</sup> Naoya Kanazawa,<sup>6</sup> Yoshinori Tokura,<sup>4, 6</sup> Stefan Blügel,<sup>3</sup> and  
Rafal E. Dunin-Borkowski<sup>1</sup>

<sup>1)</sup>*Ernst Ruska-Centre for Microscopy and Spectroscopy with Electrons  
and Peter Grünberg Institute, Forschungszentrum Jülich, 52425 Jülich,  
Germany*

<sup>2)</sup>*Donetsk Institute for Physics and Engineering, National Academy of Sciences of  
Ukraine, 03028 Kyiv, Ukraine*

<sup>3)</sup>*Peter Grünberg Institute and Institute for Advanced Simulation,  
Forschungszentrum Jülich and JARA, 52425 Jülich, Germany*

<sup>4)</sup>*RIKEN Center for Emergent Matter Science (CEMS), Wako 351-0198,  
Japan*

<sup>5)</sup>*Institute of Physics, Chinese Academy of Sciences, 100190 Beijing,  
China*

<sup>6)</sup>*Department of Applied Physics, The University of Tokyo, Tokyo 113-8656,  
Japan*

(Dated: 10 October 2017)

---

<sup>a)</sup>Electronic mail: a.kovacs@fz-juelich.de

<sup>b)</sup>Electronic mail: n.kiselev@fz-juelich.de

## I. MODEL-BASED ITERATIVE MAGNETIZATION RECONSTRUCTION

The in-plane magnetization in the projection direction,  $\mathbf{M}_{xy}$ , was reconstructed from experimental magnetic phase images recorded using off-axis electron holography. Following the Aharonov-Bohm equation, the magnetic properties of the specimen are encoded in magnetic phase images according to the equation expression<sup>1,2</sup>

$$\varphi_{\text{mag}}(x, y) = -\frac{\mu_0}{2\Phi_0} \int \frac{(y - y') \cdot M_{\text{pr},x} - (x - x') \cdot M_{\text{pr},y}}{(x - x')^2 + (y - y')^2} dx' dy' , \quad (\text{S1})$$

where  $M_{\text{pr},x}$  and  $M_{\text{pr},y}$  are the projected components of the in-plane magnetization  $\mathbf{M}_{\text{pr}}$ ,  $\mu_0$  is the vacuum permeability and  $\Phi_0 = \frac{\pi\hbar}{e}$  is the magnetic flux quantum. The projected in-plane magnetization,  $\mathbf{M}_{xy}$ , can be obtained by dividing  $\mathbf{M}_{\text{pr}}$  by the sample thickness  $t$ . This equation describes the forward problem of calculating the magnetic phase shift from a given in-plane magnetization distribution and can be expressed in matrix form as:

$$\mathbf{y} = \mathbf{F} \cdot \mathbf{x}, \quad (\text{S2})$$

where  $\mathbf{y}$  is a measurement vector containing the vectorized form of the magnetic phase image,  $\mathbf{x}$  is a magnetic state vector containing the retrieval targets (*i.e.*,  $\mathbf{M}_{xy}$  in vectorized form) and  $\mathbf{F}$  is the system matrix, which is used to apply the convolutions described in Eq. 1.

The inverse problem of retrieving the in-plane magnetization distribution from a measured magnetic phase image is ill-posed, *i.e.*, a solution for  $\mathbf{M}_{xy}$  may not exist, or, if it does, it may not be unique<sup>3</sup>. The ill-posed nature of the problem makes direct inversion of Eq. 2 impossible, as  $\mathbf{F}$  is a rank-deficient matrix.

The inverse problem is solved here by applying a model-based iterative reconstruction (MBIR) algorithm. In a first step, the ill-posed problem is approximated by a least squares minimization, which guarantees the existence of a solution. In order to enforce the uniqueness of the solution, Tikhonov regularization<sup>4</sup> of first order is employed to apply smoothness constraints to the reconstructed magnetization distribution. This approach is motivated by the minimization of the exchange energy of the system, which is also proportional to the first spatial derivatives of the magnetization distribution<sup>5</sup>. The number of retrieval targets is reduced by using *a priori* knowledge about the size and position of the magnetized regions in the form of a two-dimensional mask. The MBIR algorithm allows for the fitting of an

arbitrary ramp and offset, which may be present due to specimen charging, changes to the biprism wire over time or magnetization sources outside the field of view.

All of these measures can be included in a cost function, whose minimisation replaces the original ill-posed problem in the form

$$C(\mathbf{x}) = \|\mathbf{F}\mathbf{x} - \mathbf{y}\|_{\mathbf{S}_\epsilon}^2 - \lambda \|\mathbf{x}\|_{\mathbf{S}_a}^2, \quad (\text{S3})$$

The first Euclidean norm describes the compliance of the simulated phase image with the measurements and is weighted by a covariance matrix  $\mathbf{S}_\epsilon$  which can be used to exclude parts of the phase image from the reconstruction process. The second Euclidean norm operates solely on the magnetic state vector and is weighted by a matrix  $\mathbf{S}_a$ , which facilitates Tikhonov regularization. Both terms are balanced against each other by using a regularization parameter  $\lambda$ . Minimization of the cost function is achieved iteratively by using a conjugate gradient algorithm. In order to guarantee efficiency of the model-based reconstruction, the forward model implementation was optimized for fast and accurate simulations of magnetic phase images by employing fast convolutions in Fourier space with pre-calculated convolution kernels based on known analytic solutions for the phase contributions of simple geometries in real space.

## II. DEFOCUSED LORENTZ (FRESNEL) IMAGE INTENSITY OF A SKYRMION LATTICE

Lorentz (Fresnel) images are defocused TEM images, which are often recorded with the sample in magnetic-field-free conditions. Figure S1 shows representative defocused Lorentz images of a lattice of Bloch-type skyrmions. A qualitative description of the recorded contrast is based on the fact that the Lorentz force gives rise to deflections of the electron beam, resulting in the formation of local maxima or minima in intensity at the positions of magnetic domain walls. In a lattice arrangement, in which all of the skyrmions have the same chirality, a single maximum or minimum in intensity is formed at the position of each skyrmion and the sign of the contrast changes from underfocus to overfocus, as shown in Fig. S1. The linescans shown in Fig. S1 demonstrate the fact that, for larger values of defocus, the contrast recorded underfocus is not strictly complementary to that recorded overfocus, as a result of electron interference effects.

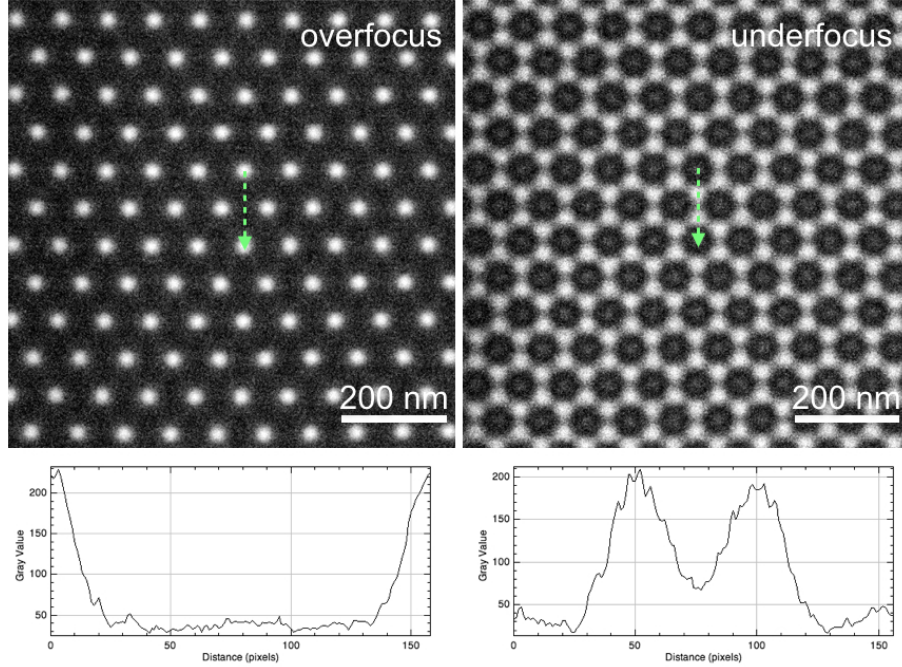


FIG. S1. Defocused Lorentz TEM images of an FeGe skyrmion lattice recorded at 200 K in the presence of a 100 mT magnetic field. Arrows indicate the positions of the corresponding intensity linescans.

## REFERENCES

- <sup>1</sup>R. E. Dunin-Borkowski, T. Kasama, A. Wei, S. L. Tripp, M. J. Hytch, E. Snoeck, R. J. Harrison, and A. Putnis, *Microscopy Research and Technique* **64**, 390 (2004).
- <sup>2</sup>M. Mansuripur, *Journal of Applied Physics* **69**, 2455 (1991).
- <sup>3</sup>H. W. Engl, M. Hanke, and A. Neubauer, *Regularization of inverse problems* (Kluwer Academic Publishers, Dordrecht and Boston, 1996).
- <sup>4</sup>A. N. Tikhonov and V. I. Arsenin, *Solutions of Ill-Posed Problems*, Scripta series in mathematics (Winston and Distributed solely by Halsted Press, Washington and New York, 1977).
- <sup>5</sup>K. M. Krishnan, *Fundamentals and Applications of Magnetic Materials*, 1st ed. (Oxford University Press, Oxford, United Kingdom, 2016).